Cell Reports
Methods

Report

A fast, aqueous, reversible three-day tissue clearing method for adult and embryonic mouse brain and whole body

Graphical abstract

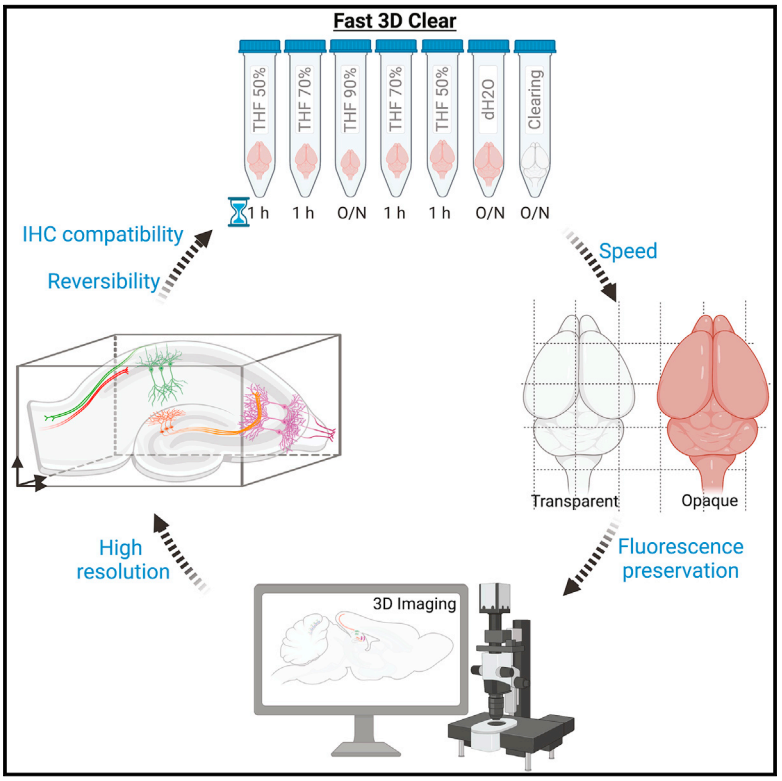

Authors

Stylianos Kosmidis, Adrian Negrean, Alex Dranovsky, Attila Losonczy, Eric R. Kandel

Correspondence

erk5@columbia.edu (E.R.K.), sk3440@columbia.edu (S.K.)

In brief

Tissue clearing enables the study of cells as units and as components of a network within intact organs. Kosmidis et al. develop an easy and speedy method for clearing large tissues and visualizing individual cells and their connections within the brain in 3D.

Highlights

- Fast 3D Clear is a method for large tissue clearing and 3D imaging
- The method is simple, inexpensive, and reversible
- Tissue size and endogenous fluorescence are preserved
- Fast 3D Clear enables the study of neuronal structure and connectivity

Kosmidis et al., 2021, Cell Reports Methods *1*, 100090
November 22, 2021
https://doi.org/10.1016/j.crmeth.2021.100090

CellPress

Cell Reports Methods

CellPress
OPEN ACCESS

Report

A fast, aqueous, reversible three-day tissue clearing method for adult and embryonic mouse brain and whole body

Stylianos Kosmidis,[1,3,4,*] Adrian Negrean,[1,3] Alex Dranovsky,[5] Attila Losonczy,[1,2,3] and Eric R. Kandel[1,2,3,4,6,*]
[1]Zuckerman Mind Brain Behavior Institute, Columbia University, New York, NY 10027, USA
[2]Kavli Institute for Brain Science, Columbia University, New York, NY 10027, USA
[3]Department of Neuroscience, Columbia University, New York, NY 10027, USA
[4]Howard Hughes Medical Institute, Columbia University, New York, NY 10027, USA
[5]New York State Psychiatric Institute, New York, NY 10032, USA; Department of Psychiatry, Columbia University, New York, NY 10032, USA
[6]Lead contact
*Correspondence: erk5@columbia.edu (E.R.K.), sk3440@columbia.edu (S.K.)
https://doi.org/10.1016/j.crmeth.2021.100090

MOTIVATION Whole-tissue clearing has become an indispensable approach to study the morphology and connectivity of the nervous system. Here, we describe Fast 3D Clear, a clearing method that integrates simplicity, speed, versatility, and high transparency, without sacrificing safety, tissue integrity, and the preservation of endogenous fluorescence.

SUMMARY

Optical clearing methods serve as powerful tools to study intact organs and neuronal circuits. We developed an aqueous clearing protocol, Fast 3D Clear, that relies on tetrahydrofuran for tissue delipidation and iohexol for clearing, such that tissues can be imaged under immersion oil in light-sheet imaging systems. Fast 3D Clear requires 3 days to achieve high transparency of adult and embryonic mouse tissues while maintaining their anatomical integrity and preserving a vast array of transgenic and viral/dye fluorophores. A unique advantage of Fast 3D Clear is its complete reversibility and thus compatibility with tissue sectioning and immunohistochemistry. Fast 3D Clear can be easily and quickly applied to a wide range of biomedical studies, facilitating the acquisition of high-resolution two- and three-dimensional images.

INTRODUCTION

Since tissue clearing was first described over a century ago (Spalteholz, 1914; Steinke and Wolff, 2001), several optical clearing techniques have been introduced that eliminate labor-intensive histological sectioning and facilitate studies on neuronal development, morphology, and connectivity.

Clearing methods can be categorized as organic-solvent based (i.e., 3DISCO [Erturk et al., 2012], iDISCO [Renier et al., 2014], uDISCO [Pan et al., 2016], FDISCO [Qi et al., 2019], FluoClearBABB [Schwarz et al., 2015], PEGASOS [Jing et al., 2018]) or aqueous (i.e., CLARITY [Chung and Deisseroth, 2013], PACT-PARS [Yang et al., 2014], CUBIC [Tainaka et al., 2014]). Organic-solvent-based protocols provide high-level tissue transparency in 3–4 days, with the exception of FluoClearBABB, which requires 10 days. The main disadvantages of these protocols include bleaching of fluorescent protein labels (3DISCO), long antibody incubation times (iDISCO), complexity in their operation (uDISCO), toxicity of some organic solvents, and tissue shrinkage that can impede high-resolution imaging (FDISCO). On the other hand, aqueous methods are simple in their application and can preserve fluorescent proteins. However, these protocols often require specific equipment (CLARITY), and the clearing process is lengthy (CUBIC, PACT-PARS).

We have built upon these powerful techniques to develop an alternative method of whole-tissue clearing, Fast 3D Clear. Fast 3D Clear results in highly transparent adult and embryonic mouse tissue within 3 days, requiring only four solutions and seven steps. The refractive index (RI)-matching aqueous clearing and imaging solution formulation does not produce toxic vapors and is compatible with standard microscopy and optics. The tissue morphology and size are not compromised, whereas endogenous fluorescent labels with emission spanning from blue to far red are preserved for several months. The clearing procedure of Fast 3D Clear is reversible, as tissues can be returned to their previous non-transparent state and are suitable for further processing with immunohistochemistry/immunofluorescence.

RESULTS

Fast 3D Clear achieves high tissue transparency in brains, whole adult mice, and embryos

Fast 3D Clear consists of seven steps and requires 3 days to achieve complete transparency (Figure 1A). Tissue dehydration/delipidation relies on tetrahydrofuran (THF) (Erturk et al., 2012), which can rapidly infiltrate and conserve soft tissues (Haust, 1959). To avoid bleaching of genetically expressed reporters, we used THF at pH 9–9.5, which reduces fluorescence quenching (Qi et al., 2019). To further avoid deterioration of fluorescence and overall tissue integrity (i.e., shrinkage), as happens with the use of organic solutions (100% THF), we reversed THF-induced dehydration by gradually decreasing the THF concentration to water, leading to complete restoration of tissue size (Figures 1B and 1C). Prolonged washing of the brain with dH_2O water after THF treatment causes a linear expansion of the tissue compared with its original size (Figures S1A and S1E). To maintain tissue expansion along with the fluorescence, we incorporated urea into the iohexol-based clearing solution (Figures 1D and S1C–S1E). We used this aqueous clearing solution to preserve and visualize the cleared tissue in an RI-matched non-toxic Cargille type A immersion oil with RI = 1.515. Fast 3D Clear resulted in intact, highly transparent adult mouse brains (Figures 1C and 1D) compared with fixed brains (Figures 1B and S1B). We next tested Fast 3D Clear in whole adult mice and mouse embryos. Fast 3D Clear was able to produce sufficiently transparent embryonic day (E) 18.5 mouse embryos and post-natal day (P) 24, 1-month, and 3-month adult whole mice (Figures 1E–1I), as well as whole soft organs (Figures S1F–S1I), while maintaining fluorescence without affecting the background (Figures S1J–S1N). Thus, Fast 3D Clear is a simple procedure that leads to high transparency in a wide variety of tissues, including the central nervous system.

Comparison of Fast 3D Clear with other clearing methods

To assess its efficiency and simplicity, we subjected brain hemispheres derived from the same animal to Fast 3D Clear and FDISCO, or Fast 3D Clear and RTF (Figures 1J, 1K, and S1O). We observed superior clearing by Fast 3D Clear compared with RTF and similar transparency compared with FDISCO. There was no noticeable difference in the visual transparency of the cleared tissue when transferred from the aqueous clearing solution to Cargille immersion oil (Figure 1J). However, there were considerable differences in the size of tissue cleared with Fast 3D Clear versus FDISCO (Figure 1J-L). Whereas FDISCO shrinks the tissue, Fast 3D Clear might lead to tissue expansion (Figure S1P) and therefore might provide higher magnification of the region of interest. We also used wintergreen oil as an imaging medium, with RI of 1.536 (Figure 1M). Although wintergreen oil led to tissue transparency similar to that of Cargille oil, it disintegrated the plastic holders. Nevertheless, our results highlight the potential compatibility of Fast 3D Clear with other commercially available immersion oils with higher RI. We next tested whether there were differences between Fast 3D Clear and FDISCO in fluorescence preservation, light transmittance, and background fluorescence, using brains from GCaMP3-CaMK2-Cre transgenic animals (Tsien et al., 1996; Zariwala et al., 2012). Using confocal (Figures 1N, 1P, and S1R–S1S) and light-sheet microscopy (Figures 1O and 1Q), we measured the signal-to-noise ratio (SNR) by using 525/50-nm laser excitation. Although the light transmittance was similar (Figure 1R), Fast 3D Cleared hemispheres had a higher SNR (Figures 1S and S1Q) than the FDISCO counterparts. Importantly, Fast 3D Clear was able to preserve the fluorescence signal, similar to that obtained with traditional immunohistochemistry (Figures S1T–S1W), and the GCaMP3 signal was preserved for a year in Cargille immersion oil (Figures S1X–S1Z).

Fast 3D Clear preserves endogenous fluorescence in adult mouse brains, whole adult mice, and embryos

To test whether Fast 3D Clear can preserve the fluorescence of common fluorescent proteins, we applied it to four transgenic mouse lines: (1) Thy1-GFP-M, characterized by high levels of GFP expression in sparse neuronal populations (Ariel, 2017); (2) GCaMP3-CaMK2-Cre (Tsien et al., 1996; Zariwala et al., 2012), in which GCaMP3 calcium-sensitive fluorescent protein is expressed in $CaMK2^+$ neurons; (3) tdTomato-VGAT-Cre (Kaneko et al., 2018), in which tdTomato is expressed in inhibitory neurons; and (4) $cFos\text{-}Cre^{ERT2}$-tdTomato (Guenthner et al., 2013), in which tamoxifen administration results in tdTomato labeling of neurons active during a behavioral task. In all four transgenic lines, adult brains became completely transparent while maintaining their corresponding fluorescence. Specifically, $Thy1\text{-}GFP^+$ neurons and $GCaMP3^+$ CaMK2 neurons were visualized in the dorsal hippocampus and ventral dentate gyrus (DG) (Figures 2A–2D) and in other cortical regions (Figures S2A–S2C). The labeling intensity of inhibitory VGAT $tdTomato^+$ neurons was lower in the dorsal hippocampus and in the DG compared with Thy1-GFP and GCaMP3-CaMK2-Cre (Figures 2E and 2F). After fear conditioning, tdTomato expression was visualized in $cFos^+$ hippocampal cell bodies and dendrites (Figures 2G and 2H). When Fast 3D Clear was applied to whole adult GCaMP3-CaMK2-Cre mice, we could visualize GCaMP3 in the mouse retina, olfactory bulb, and spinal cord (Figures S2D–S2F).

Similarly, we applied Fast 3D Clear to E18.5 mouse embryos by using the $Msx1\text{-}Cre^{ERT2}$-tdTomato transgenic mouse line. Confocal microscopy revealed tdTomato labeling in the eye (Figure S2G) and spinal cord (Figures S2H and S2I) according to Msx1 expression (Duval et al., 2014; Monaghan et al., 1991). Because some tissues can exhibit high autofluorescence (Croce and Bottiroli, 2014), we visualized the retina (Figures S2J–S2L) and the spinal cord (Figures S2M–S2O) of GCaMP3-CaMK2-Cre mice simultaneously at 405-, 488-, and 568-nm wavelengths (with corresponding emission filters 450/25, 500/30, and 585/15) by using confocal microscopy. Fast 3D Clear resulted in minimum autofluorescence in the lens of the eye and in the spinal cord, and absence of signal at 405 and 568 nm. These data illustrate that Fast 3D Clear is an optimal approach when maintaining endogenous fluorophores is critical.

Fast 3D Clear preserves the fluorescence of synthetic and genetically encoded labels at multiple emission wavelengths

To examine whether Fast 3D Clear can preserve non-endogenous fluorescence of various wavelengths, we delivered fluorescent

CellPress
OPEN ACCESS

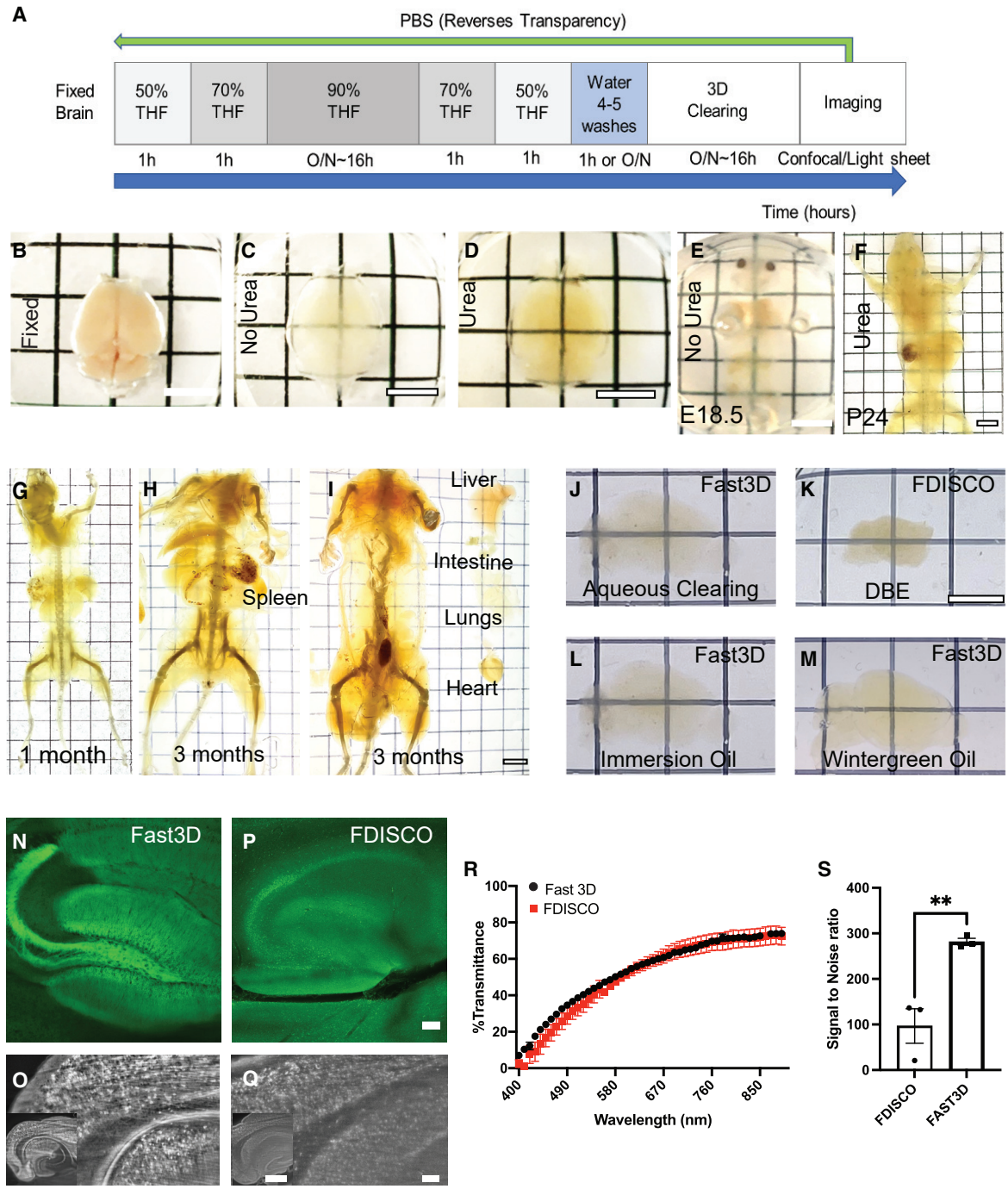

Figure 1. Overview of Fast 3D Clear

(A) Schematic of the Fast 3D Clear process.

(B–D) Transparency of adult mouse brains in Cargille oil.

(E–I) Whole cleared mouse embryo and adult mouse.

(J–M) Sagittal images of brain hemispheres subjected to Fast 3D Clear in (J) aqueous clearing solution, (L) Cargille oil, or (M) wintergreen oil or to (K) FDISCO in DBE.

(N–Q) Confocal (N and P) and light-sheet (O and Q) images from GCaMP3-CaMK2 paired hemispheres cleared with Fast 3D Clear (N and O) or FDISCO (P and Q).

(R) Comparison of light transmittance in brain hemispheres cleared with Fast 3D Clear and FDISCO, two-way ANOVA, $F(1, 4) = 1.082$, $p = 0.3571$.

(S) SNR of Fast 3D Clear and FDISCO cleared CaMK2-GCaMP3 hemispheres. Unpaired t test, $^{**}p = 0.0088$. Scale bars, 6 mm, 200 μm, 100 μm.

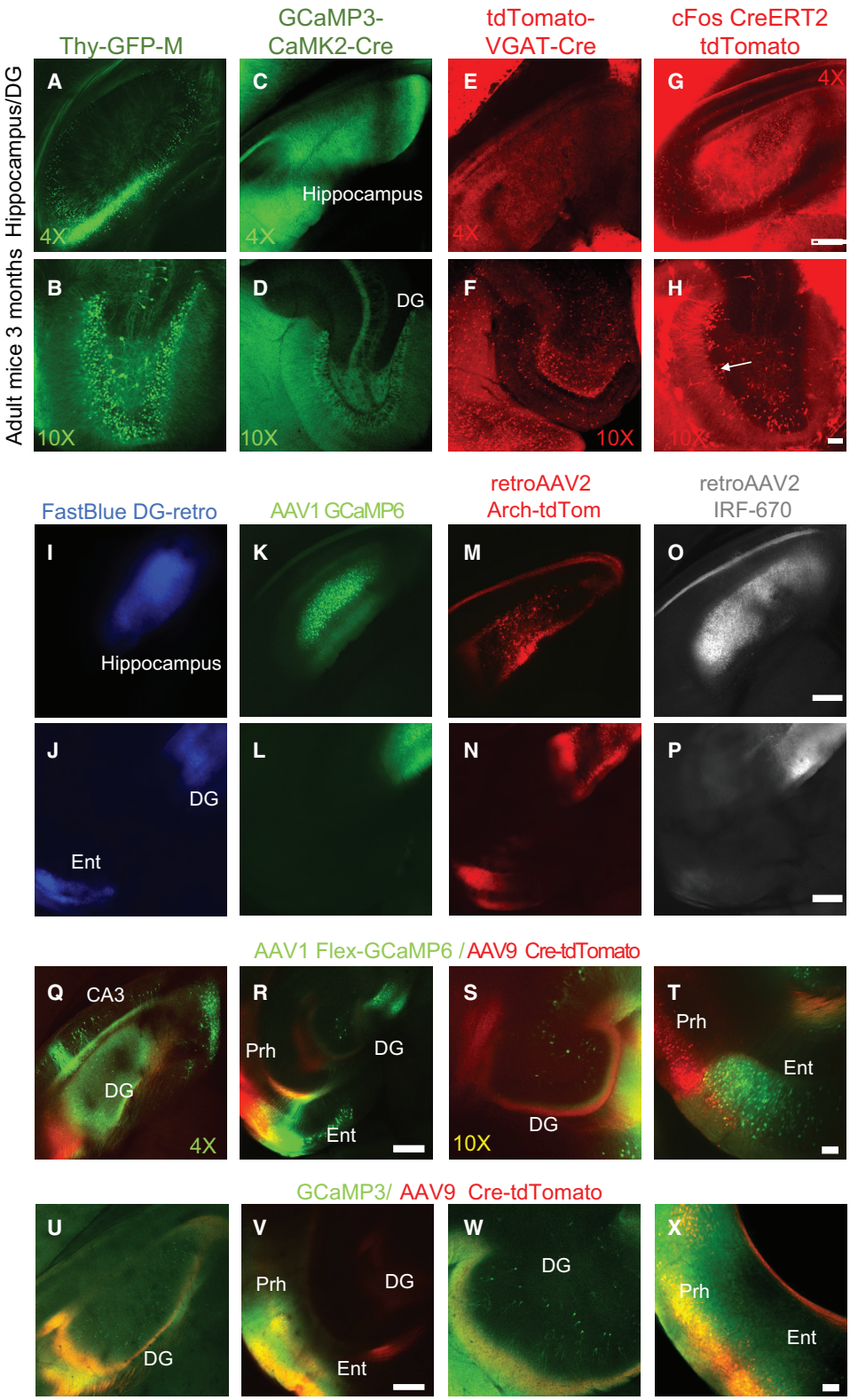

Figure 2. Fast 3D Clear preserves fluorescence in transgenic mouse brains and embryos

(A–H) Confocal images showing a dorsal view of the hippocampus of (A and B) Thy1-GFP-M, (C and D) GCaMP3-CaMK2-Cre, and (E and F) VGAT-Cre-tdTomato mice, and (G and H) cFos-Cre^{ERT2}-tdTomato mice after fear conditioning and tamoxifen administration.

(legend continued on next page)

dyes or virally expressed fluorescent proteins to the DG of the adult mouse hippocampus. Intracranial administration of the retrograde neuronal tracer Fast Blue labeled nuclei in the DG and entorhinal cortex (Ent), a brain region known to provide direct inputs to the DG (Witter et al., 2017) (Figures 2I, 2J, and S2P). Administration of AAV1 CaMK2-GCaMP6 or retro-AAV2 Arch-tdTomato viruses into the DG showed that GFP and tdTomato fluorescent proteins can be preserved and visualized in intact adult mouse brains (Figures 2K–2N, S2Q, and S2R). Next, we created a retrograde virus expressing an infrared fluorophore (IRF670). Fast 3D Clear was able to preserve the infrared fluorescence in adult mouse brains (Figures 2O, 2P, and S2S). We also measured the signal of each fluorophore from intact adult mouse brains, simultaneously, at standard excitation wavelengths (405, 488, 568, and 647 nm) with corresponding emission filters (450/25, 500/30, 585/15, and 650 IF) by using the same imaging settings for all brains. Each fluorophore generated signal restricted almost exclusively to its expected emission band (high SNR), while there was minimal fluorescence signal detected out of band through the other filters (low SNR) (Figures S2T–S2X).

Recently, Zingg et al. discovered that adeno-associated viruses (AAVs) exhibit anterograde transsynaptic labeling properties (Zingg et al., 2017), and can thus be used for tracing and visualizing neural circuits in a cell-type- and input-specific manner. To expand the application of Fast 3D Clear in neurobiology and its utility for studying neural circuits, we injected a Cre-dependent AAV1-GCaMP6 (Ding et al., 2014) virus into the dorsal hippocampus and a tdTomato-Cre-virus into the ventral Ent/perirhinal (Prh) cortex to assess whether an anterograde transfer of AAV will activate the Cre-dependent expression of GCaMP6 in the dorsal hippocampus. Three weeks later, in Fast 3D Clear-processed tissue, we observed simultaneous preservation of both GCaMP6 and tdTomato (Figures 2Q–2T). Similar results were obtained when we injected the same tdTomato-Cre adenovirus into the ventral Ent/Prh of GCaMP3 mice (Figures 2U–2X). We further applied Fast 3D Clear to CaMK2-Cre animals injected in the CA3 hippocampal subregion with a double inverted AAV encoding a designer receptor (Gq-mCherry) exclusively activated by designer drug (DREADD) technology (clozapine-N-oxide, or CNO) (Zhu and Roth, 2014)—a valuable tool to study the function of neuronal circuits, demonstrating the compatibility of Fast 3D Clear with the mCherry fluorophore (Figures S2Y and S2Z). Last, we found that Fast 3D Clear can preserve fluorescent cholera toxin subunit B (CTB). Twenty-four hours after injection into the mouse hippocampus, CTB can be clearly traced into the Ent (Figure S2AA). The compatibility of Fast 3D Clear with synthetic and genetically encoded fluorescent labels over a broad spectral range makes it an ideal method to study the structure and function of neuronal circuits.

Fast 3D Clear is compatible with light-sheet and confocal microscopy

Using light-sheet microscopy, we visualized cleared brains from the transgenic lines described above. We show that Thy1-GFP-M mouse brains and CaMK2-GCaMP6-injected brains can be imaged with sufficient resolution at the cellular level (Figures 3A–3C, Video S1). In addition, we achieved comparable cellular resolution of GCaMP3, despite it being a weaker fluorophore than Thy1-GFP (Figures 3D and 3E). Furthermore, we visualized three-dimensionally the cleared brains of cFos-Cre^{ERT2}-tdTomato and VGAT-tdTomato transgenic lines, as well as the spinal cord from Msx1-tdTomato mouse embryos (Figures 3F–3H). Using Imaris software, we visualized cleared brains in three dimensions without great compromises to morphology (Figures S3A–S3C).

We next injected mouse DG with different adenoviruses and processed the brains with Fast 3D Clear (Figures 3I–3K). In addition to the injected DG, fluorescence was preserved in retrogradely labeled neurons, and allowed high-resolution 3D imaging of structures known to project to the DG, including the Ent, medial septum, mammillary bodies, and projection neurons from the contralateral DG. We also visualized individual IRF670 hilar cells, with light-sheet (Figure 3K, Video S2) and confocal microscopy (Figures S3D and S3E). Moreover, we detected cFos^{+} in the DG (Figure S3F) and Arch-tdTomato (Figure S3G), as well as the fine processes of neurons in the CA3 region of the intact mouse hippocampus and retrosplenial cortex after GCaMP6 viral injection (Figures S3H and S3I). We also injected the IRF670 virus into the dysgranular zone (S1DZ) of the somatosensory cortex and visualized cortical areas projecting to S1DZ, such as the rostrolateral area (RL), anterior area (A), and anteromedial area (AM) (Figure 3L). In addition, we could trace in 3D the Ent-DG neuronal circuit by using light sheet (Figure 3M) or a spinning-disk confocal microscope (Figure S3J). To verify the specificity of the labeling, we also processed unlabeled brains of wild-type mice. We found that Fast 3D Clear resulted in minimum background fluorescence (Figures S3K–S3M). Finally, Fast 3D Clear allowed us to detect three-dimensionally fine neuronal processes (spines) in the insular and retrosplenial cortex of Thy1-GFP-M mouse brains, by using a 20× lens with high NA (0.95) (Figures 3N, 3O, S3N, and S3O, Video S1). In summary, Fast 3D Clear is fully compatible with both specialized and simple microscopy instruments, and it provides an efficient solution to 3D imaging of the intact mouse brain.

Fast 3D Clear is compatible with fluorescent antibody labeling

After Fast 3D Clearing, transparent mouse brains were returned to their initial opaque state (see STAR Methods). cFos-Cre^{ERT2}-tdTomato-labeled and cleared brain sections were indistinguishable from non-Fast 3D Clear processed brains in terms of both

(I–P) Fluorescence images of whole adult brains scanned at the same plane displaying the hippocampal formation (top) and the DG and Ent (bottom), from wild-type (WT) animals injected with (I and J) Fast Blue, (K and L) AAV1 GCaMP6-CaMK2, (M and N) rAAV2 Arch-tdTomato, or (O and P) rAAV2 IRF670.
(Q–X) Shown in (Q)–(T) are the dorsal hippocampus and Ent/Prh labeled with GFP and tdTomato after injection of AAV1 GCaMP6 and tdTomato-Cre virus into WT mice. (Q) Hippocampal formation, (R) entorhinal cortex and dentate gyrus. (S) 10X magnification of dentate gyrus and (T) perirhinal/entorhinal cortex. Shown in (U-X) is the injection of tdTomato-Cre virus into GCaMP3 mice. (U) Hippocampal formation, (V) entorhinal cortex and dentate gyrus. (W) 10X magnification of dentate gyrus and (T) perirhinal/entorhinal cortex. Scale bars, 200 μm for 4× and 80 μm for 10× magnification.

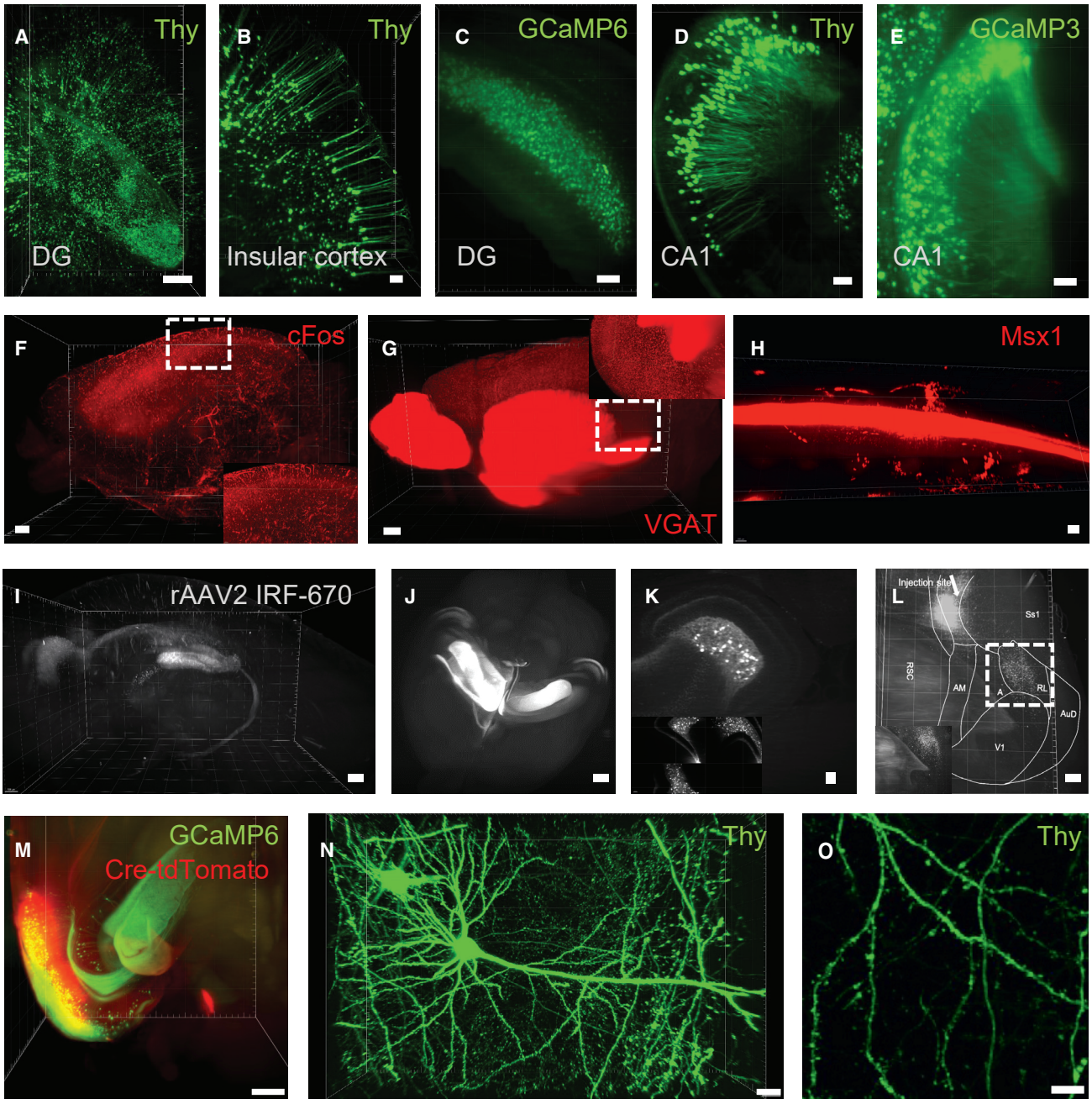

Figure 3. Fast 3D Clear is compatible with light-sheet and confocal microscopy

(A and B) Light-sheet images from Thy1-GFP animals in (A) hippocampus and (B) cortex.

(C) Light-sheet imaging of CaMK2-GCaMP6 injection in the DG.

(D and E) CA1 region of (D) Thy1-GFP and (E) GCaMP3-CaMK2 animals.

(F–H) 3D visualization of cleared (F) cFos-Cre^{ERT2}-tdTomato brain, (G) VGAT-Cre-tdTomato, and (H) spinal cord from Msx1-Cre^{ERT2}-Tdtomato E18.5 mouse embryos.

(I) 3D reconstruction of a whole adult mouse brain injected unilaterally with retro-AAV2 IRF670 and imaged with light-sheet microscopy (2× sagittal view).

(J) Different brain with retro-AAV2 IRF670 (top view).

(K) 12× magnification image from the same brain as in (J).

(L) Injection of retro-AAV2 IRF670 into the S1DZ brain regions showing retro-labeled cells.

(M) Light-sheet 3D reconstruction from animals injected with tdTomato-Cre (EC/Prh) and GCaMP6 (DG) virus.

(N) 3D reconstruction of cortical neuron from Thy1-GFP animal showing dendritic spines.

(O) Digital zoom from the same neuron in (N) showing spines. Scale bars, (A) 1,000 μm, (C) 700 μm, (F, G, J, L) 500 μm, (B, E, H, M) 200 μm, (D) 100 μm, (K, N) 20 μm, (O) 10 μm.

CellPress
OPEN ACCESS

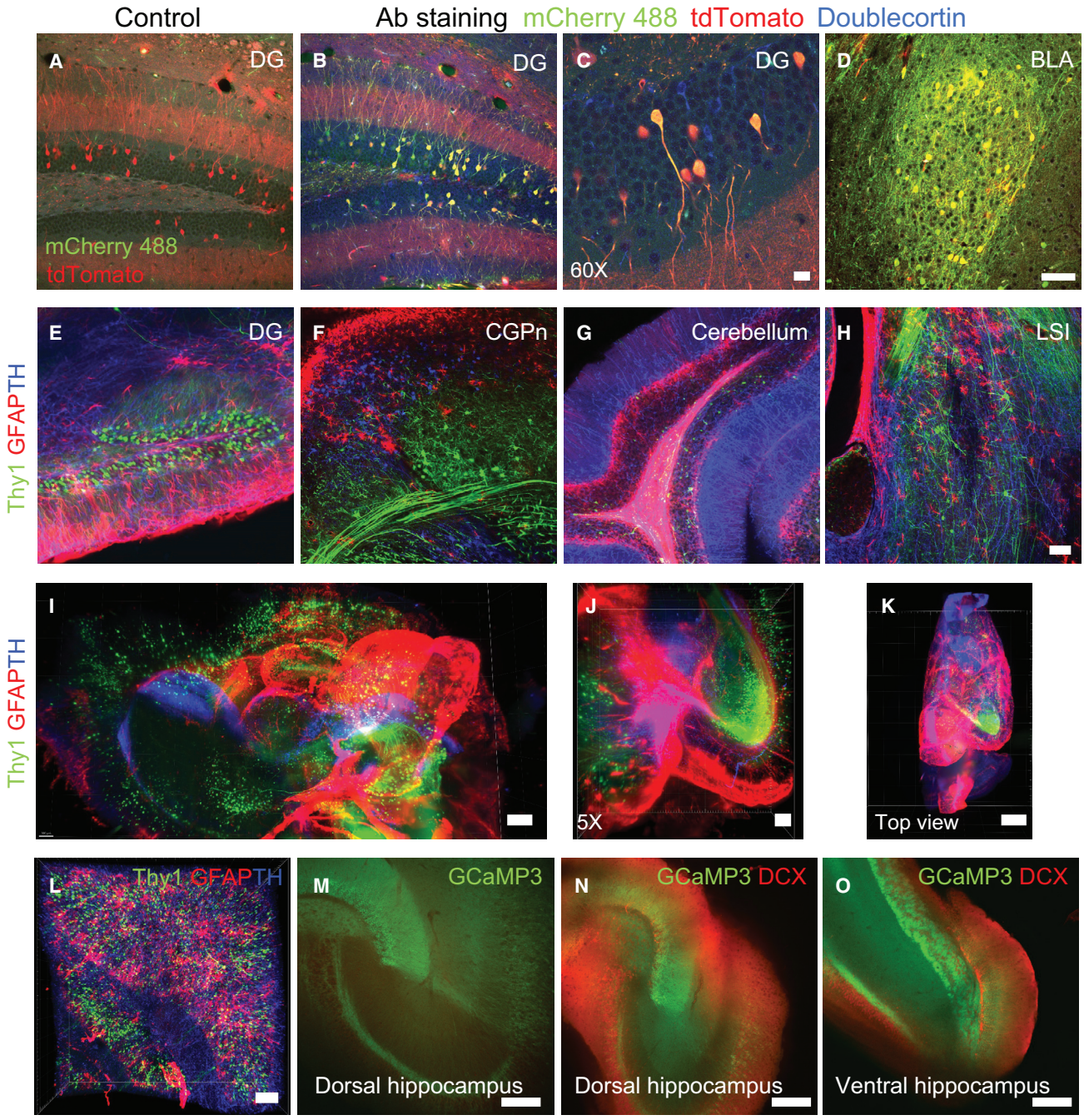

Figure 4. Fast 3D Clear is reversible and compatible with antibody staining

Brain sections after reverse clearing.

(A) Sections from cFos-Cre^{ERT2}-tdTomato animals incubated with only Alexa 488 and 647 secondary antibodies. Only the endogenous tdTomato can be detected.

(B–D) Sections from the same animals stained with antibodies against (B) mCherry (488), (C) tdTomato, and (D) doublecortin (DCX) (647). DCX staining is completely absent from the basolateral amygdala (BLA).

(E–H) Confocal images from the (E) DG, (F) central gray of the pons (CGPn), (G) cerebellum, and (H) lateral septum (LSI) of Thy1-GFP half-brains stained with GFAP and TH antibodies.

(I–K) 3D visualization (light sheet) from Thy1-GFP half-brains stained with GFAP and TH.

(L) 3D visualization of cerebellum from Thy1-GFP half-brain stained with GFAP and TH using confocal microscopy.

(legend continued on next page)

tdTomato fluorescence and overall neuronal structure (Figures 4A and 4B). Fast 3D Clear did not hinder the detection of antigens, as demonstrated by the detection of mCherry in the DG (Figures 4A and 4B) and doublecortin in the DG, basolateral amygdala (BLA), and Ent/Prh (Figures 4B–4D and S4A–S4D).

To test whether Fast 3D Clear is compatible with immunostaining in larger tissue volumes, we cleared brain hemispheres from Thy1-GFP-M mice. After detecting Thy1-GFP$^+$ cells, we reversed the tissue transparency and subjected the samples to an iDISCO staining protocol by using antibodies against tyrosine hydroxylase (TH) and glial fibrillary acidic protein (GFAP) (see STAR Methods). Antibody staining was followed by sample incubation in the Fast 3D Clearing solution until full transparency was reached. Fast 3D Clear allowed the preservation of endogenous Thy1-GFP fluorescence, as expected, as well as simultaneous tissue staining for GFAP and TH (Figures 4E–4L, Video S3). We also used GCaMP3-CaMK2 animals and subjected them to a shorter Fast 3D Clear protocol (see STAR Methods). The clearing process was reversed, and hippocampi were stained for doublecortin by using a short iDISCO protocol (Renier et al., 2016). Although iDISCO caused a small increase in the background fluorescence, we were able to visualize GCaMP3$^+$ neurons and doublecortin$^+$ neurons in the DG (Figures 4M–4O, S4E, and S4F). Collectively these data demonstrate that Fast 3D Clear can be compatible with iDISCO staining.

DISCUSSION

Three-dimensional imaging of cleared tissues has revolutionized neuroscience research, enabling the visualization of single neurons at high resolution and their assembly into circuits in the intact central nervous system. A wide variety of clearing protocols have become available, and several factors need to be taken into account for choosing the most appropriate approach. These deciding factors include time, cost, complexity, safety, model organism, preservation of fluorophores, and experimental question (Ariel, 2017). Here we describe Fast 3D Clear, a clearing method that is compatible with various fluorescent proteins, synthetic dyes, and antibody labeling (Table S1). The first benefit of Fast 3D Clear is speed, comparable to that of sDISCO (Hahn et al., 2019) and FDISCO. Intact adult mouse brains, peripheral organs, mouse embryos, and entire young adult mice become transparent in just 3 days. Fast 3D Clear is better suited to screening purposes, given that it is considerably faster compared with CLARITY, iDISCO, FluoClearBABB, CUBIC, PEGASOS, and PACT. Second, Fast 3D Clear is cost effective. It does not require specialized equipment, as CLARITY does, and the necessary reagents are only minimal, compared with those required by CLARITY, iDISCO, FluoClearBABB, and PEGASOS. In addition, Fast 3D Clear reagents are inexpensive and their commercially available quantities are adequate for multiple samples. Another positive feature of Fast 3D Clear is that it is simple. The protocol includes a limited number of simple incubation steps with THF, which does not require a special process to remove reactive oxygen species and is not an immediate hazardous source if handled properly (Hahn et al., 2019; Qi et al., 2019). Fast 3D Clear also overcomes the environmental hazard of dibenzyl ether (DBE) and simplifies the clearing procedure by using an aqueous clearing solution and RI-matching alternatives that do not require complete dehydration with THF. Iohexol has been used previously in RI-matching solutions and as a radiographic contrast agent, and it is an ideal clearing candidate that satisfies our environmental concerns. Moreover, aqueous solutions of high RI can be prepared with ease, matching common immersion oils or reaching close to the RI of DBE at a usable viscosity. Compared with some previously published methods (Jing et al., 2018; Qi et al., 2019), Fast 3D Clear completely overcomes tissue shrinkage. Reversal of the dehydration/delipidation THF process can restore tissue size, whereas extended incubation with water can cause tissue expansion, which can be maintained with the addition of urea without significant fluorescence loss. This moderate expansion feature of Fast 3D Clear can be beneficial particularly for the visualization of neuronal circuits. Using Fast 3D Clear, we were able to maintain the fluorescence of genetically encoded fluorescent proteins for more than a year and adequately maintain the fluorescence of weaker fluorophores such as GCaMP3. Fast 3D Clear can additionally be used in combination with antibodies to further visualize neuronal circuits. Last, Fast 3D Clear can be used to faithfully reconstruct dendrites from sparsely labeled neuronal structures.

Our future studies are to further validate Fast 3D Clear by registering the cell types in the Mouse Brain Atlas and, in parallel, perform immunohistochemistry on the same brains in order to bridge the two methods. This will provide an unprecedented strategy for registering multiple cell types in both two and three dimensions, with further applications to translational research. Last, it remains of interest to assess whether Fast 3D Clear, because of its reversibility, can be combined with other molecular processes such as fluorescence-activated cell sorting and *in situ* hybridization. In conclusion, Fast 3D Clear can be an important and practical tool with multiple and broad applications in biochemical studies and clinical diagnoses of pathological diseases in the fields of neuroscience, cancer biology, and drug screening.

Limitations of the study

Despite the strong advantages of Fast 3D Clear, further testing of some of its applications is still required. First, Fast 3D Clear has not been tested in organisms other than mice, for which other methods have demonstrated excellent results (reviewed in Tian et al., 2021). The second limitation of Fast 3D Clear is its modest ability to produce completely transparent hard tissues. Although other methods (e.g., BONE clear) (Jing et al., 2018; Wang et al., 2019) are extremely competent, Fast 3D Clear can be applied only to whole young adult mice with moderate bone clearing. Conversely, application of Fast 3D Clear to 3-month-old mice displays reduced efficiency in hard-tissue transparency (bones). It would be useful to test whether we can combine Fast 3D Clear

(M–O) Whole adult mouse hippocampus from GCaMP3-CaMK2-Cre animals cleared with Fast 3D Clear. (M) GCaMP3 fluorescence before staining, (N) fluorescence at 500/30 and 650LP nm for GCaMP3 and DCX in dorsal hippocampus, and (O) ventral hippocampus merged channels. Scale bars, (I, K) 500 μm, (J and L) 200 μm, (E, F, G, H, M, N, O) 80 μm, (A, B, D) 20 μm, (C) 5 μm.

with decalcification and discoloration solutions (as in PEGASOS and BONE clear) to produce a fully transparent adult mouse. Although Fast 3D Clear is compatible with iDISCO whole-tissue staining, we have not validated the stability of the antibody fluorescence under longer storage conditions in the Cargille oil or clearing media. We have also not used other immunostaining protocols and reagents, such as antioxidants (i.e., propyl gallate, sDISCO), to evaluate long-term storage conditions for antibody-treated tissues. Last, we have not yet confirmed the compatibility of Fast 3D Clear with a cell registration software.

STAR★METHODS

Detailed methods are provided in the online version of this paper and include the following:

- KEY RESOURCE TABLE
- RESOURCE AVAILABILITY
  - Lead contact
  - Materials availability
  - Data and code availability
- EXPERIMENTAL MODEL AND SUBJECT DETAILS
  - Animals
- METHOD DETAILS
  - Light transmittance measurements
  - Signal to noise ratio
  - Fluorescence quantification
  - Perfusion and tissue preparation
  - Fast 3D Clear protocol
  - Fast 3D Clear solution
  - FDISCO clearing
  - RTF clearing
  - Imaging
  - Immunohistochemistry
  - Immunolabeling protocol (iDISCO)
  - Tamoxifen (TAM)
  - Contextual fear conditioning in cFos-Cre^{ERT2}-tdTomato mice
  - HEK293FT cell culture, transfection, and production of rAAV2 and AAV
- QUANTIFICATION AND STATISTICAL ANALYSIS

SUPPLEMENTAL INFORMATION

Supplemental information can be found online at https://doi.org/10.1016/j.crmeth.2021.100090.

ACKNOWLEDGMENTS

We thank Dr. Carol A. Mason and Dr. Nefeli Slavi for providing us the Msx1 tdTomato embryos. The Thy1-GFP-M mouse line was a gift from Dr. Josef Gogos. Funding was provided by the Howard Hughes Medical Institute. We also thank the Advanced Instrumentation Core of the Zuckerman Institute and particularly Darcy Peterka, Luke Hammond, and Humberto Ibarra Avila for comments on the manuscript and technical assistance.

AUTHOR CONTRIBUTIONS

S.K. and A.N. developed the clearing protocol; S.K. performed experiments; S.K., A.D., A.L., and E.R.K. designed the research; S.K. wrote the manuscript with contributions from A.N., A.L., and E.R.K. S.K., A.N., A.L., and E.R.K. have filled an IR CU21159.

DECLARATION OF INTERESTS

The authors declare no competing interests. A patent has been filed by S.K., A.N., A.L., and E.R.K.' and the Zuckerman Institute.

Received: December 18, 2020
Revised: April 13, 2021
Accepted: September 3, 2021
Published: October 11, 2021

REFERENCES

Ariel, P. (2017). A beginner's guide to tissue clearing. Int. J. Biochem. Cell Biol. *84*, 35–39.

Chung, K., and Deisseroth, K. (2013). CLARITY for mapping the nervous system. Nat. Methods *10*, 508–513.

Croce, A.C., and Bottiroli, G. (2014). Autofluorescence spectroscopy and imaging: a tool for biomedical research and diagnosis. Eur. J. Histochem. *58*, 2461.

Ding, J., Luo, A.F., Hu, L., Wang, D., and Shao, F. (2014). Structural basis of the ultrasensitive calcium indicator GCaMP6. Sci. China Life Sci. *57*, 269–274.

Duval, N., Daubas, P., Bourcier De Carbon, C., St Cloment, C., Tinevez, J.Y., Lopes, M., Ribes, V., and Robert, B. (2014). Msx1 and Msx2 act as essential activators of Atoh1 expression in the murine spinal cord. Development *141*, 1726–1736.

Erturk, A., Becker, K., Jahrling, N., Mauch, C.P., Hojer, C.D., Egen, J.G., Hellal, F., Bradke, F., Sheng, M., and Dodt, H.U. (2012). Three-dimensional imaging of solvent-cleared organs using 3DISCO. Nat. Protoc. *7*, 1983–1995.

Guenthner, C.J., Miyamichi, K., Yang, H.H., Heller, H.C., and Luo, L. (2013). Permanent genetic access to transiently active neurons via TRAP: targeted recombination in active populations. Neuron *78*, 773–784.

Hahn, C., Becker, K., Saghafi, S., Pende, M., Avdibasic, A., Foroughipour, M., Heinz, D.E., Wotjak, C.T., and Dodt, H.U. (2019). High-resolution imaging of fluorescent whole mouse brains using stabilised organic media (sDISCO). J. Biophotonics *12*, e201800368.

Haust, M.D. (1959). Tetrahydrofuran (THF) for routine dehydration, clearing, and infiltration. Am. J. Clin. Pathol. *31*, 357–361.

Jing, D., Zhang, S., Luo, W., Gao, X., Men, Y., Ma, C., Liu, X., Yi, Y., Bugde, A., Zhou, B.O., et al. (2018). Tissue clearing of both hard and soft tissue organs with the PEGASOS method. Cell Res. *28*, 803–818.

Kaneko, R., Takatsuru, Y., Morita, A., Amano, I., Haijima, A., Imayoshi, I., Tamamaki, N., Koibuchi, N., Watanabe, M., and Yanagawa, Y. (2018). Inhibitory neuron-specific Cre-dependent red fluorescent labeling using VGAT BAC-based transgenic mouse lines with identified transgene integration sites. J. Comp. Neurol. *526*, 373–396.

Kosmidis, S., Polyzos, A., Harvey, L., Youssef, M., Denny, C.A., Dranovsky, A., and Kandel, E.R. (2018). RbAp48 Protein Is a Critical Component of GPR158/OCN Signaling and Ameliorates Age-Related Memory Loss. Cell Rep *25*, 959–973 e6.

Monaghan, A.P., Davidson, D.R., Sime, C., Graham, E., Baldock, R., Bhattacharya, S.S., and Hill, R.E. (1991). The Msh-like homeobox genes define domains in the developing vertebrate eye. Development *112*, 1053–1061.

Pan, C., Cai, R., Quacquarelli, F.P., Ghasemigharagoz, A., Lourbopoulos, A., Matryba, P., Plesnila, N., Dichgans, M., Hellal, F., and Erturk, A. (2016). Shrinkage-mediated imaging of entire organs and organisms using uDISCO. Nat. Methods *13*, 859–867.

Qi, Y., Yu, T., Xu, J., Wan, P., Ma, Y., Zhu, J., Li, Y., Gong, H., Luo, Q., and Zhu, D. (2019). FDISCO: Advanced solvent-based clearing method for imaging whole organs. Sci. Adv. *5*, eaau8355.

Renier, N., Adams, E.L., Kirst, C., Wu, Z., Azevedo, R., Kohl, J., Autry, A.E., Kadiri, L., Umadevi Venkataraju, K., Zhou, Y., et al. (2016). Mapping of brain

activity by automated volume Analysis of immediate early genes. Cell *165*, 1789–1802.

Renier, N., Wu, Z., Simon, D.J., Yang, J., Ariel, P., and Tessier-Lavigne, M. (2014). iDISCO: a simple, rapid method to immunolabel large tissue samples for volume imaging. Cell *159*, 896–910.

Schmidt, E., Nilsson, O., Koskela, A., Tuukkanen, J., Ohlsson, C., Rozell, B., and Eriksson, M. (2012). Expression of the Hutchinson-Gilford progeria mutation during osteoblast development results in loss of osteocytes, irregular mineralization, and poor biomechanical properties. J. Biol. Chem. *287*, 33512–33522.

Schneider, C.A., Rasband, W.S., and Elicieri, K.W. (2012). NIH Image to ImageJ: 25 years of image analysis. Nat Methods *9*, 671–675.

Schwarz, M.K., Scherbarth, A., Sprengel, R., Engelhardt, J., Theer, P., and Giese, G. (2015). Fluorescent-protein stabilization and high-resolution imaging of cleared, intact mouse brains. PLoS One *10*, e0124650.

Spalteholz, W. (1914). A Method for the Clearing of Human and Animal Specimens (S. Hirzel).

Steinke, H., and Wolff, W. (2001). A modified Spalteholz technique with preservation of the histology. Ann. Anat. *183*, 91–95.

Tainaka, K., Kubota, S.I., Suyama, T.Q., Susaki, E.A., Perrin, D., Ukai-Tadenuma, M., Ukai, H., and Ueda, H.R. (2014). Whole-body imaging with single-cell resolution by tissue decolorization. Cell *159*, 911–924.

Tian, T., Yang, Z., and Li, X. (2021). Tissue clearing technique: recent progress and biomedical applications. J. Anat. *238*, 489–507.

Tsien, J.Z., Chen, D.F., Gerber, D., Tom, C., Mercer, E.H., Anderson, D.J., Mayford, M., Kandel, E.R., and Tonegawa, S. (1996). Subregion- and cell type-restricted gene knockout in mouse brain. Cell *87*, 1317–1326.

Wang, Q., Liu, K., Yang, L., Wang, H., and Yang, J. (2019). BoneClear: whole-tissue immunolabeling of the intact mouse bones for 3D imaging of neural anatomy and pathology. Cell Res. *29*, 870–872.

Witter, M.P., Doan, T.P., Jacobsen, B., Nilssen, E.S., and Ohara, S. (2017). Architecture of the entorhinal cortex A review of entorhinal anatomy in rodents with some comparative notes. Front. Syst. Neurosci. *11*, 46.

Yang, B., Treweek, J.B., Kulkarni, R.P., Deverman, B.E., Chen, C.K., Lubeck, E., Shah, S., Cai, L., and Gradinaru, V. (2014). Single-cell phenotyping within transparent intact tissue through whole-body clearing. Cell *158*, 945–958.

Yu, T., Zhu, J., Li, Y., Ma, Y., Wang, J., Cheng, X., Jin, S., Sun, Q., Li, X., Gong, H., et al. (2018). RTF: a rapid and versatile tissue optical clearing method. Sci. Rep. *8*, 1964.

Zariwala, H.A., Borghuis, B.G., Hoogland, T.M., Madisen, L., Tian, L., De Zeeuw, C.I., Zeng, H., Looger, L.L., Svoboda, K., and Chen, T.W. (2012). A Cre-dependent GCaMP3 reporter mouse for neuronal imaging in vivo. J. Neurosci. *32*, 3131–3141.

Zhu, H., and Roth, B.L. (2014). DREADD: a chemogenetic GPCR signaling platform. Int. J. Neuropsychopharmacol. *18*, pyu007.

Zingg, B., Chou, X.L., Zhang, Z.G., Mesik, L., Liang, F., Tao, H.W., and Zhang, L.I. (2017). AAV-mediated anterograde transsynaptic tagging: mapping corticocollicular input-defined neural pathways for defense behaviors. Neuron *93*, 33–47.

STAR★METHODS

KEY RESOURCE TABLE

REAGENT or RESOURCE	SOURCE	IDENTIFIER
Antibodies		
anti-Doublecortin DCX	Millipore-Sigma	Cat# AB2253, RRID:AB_1586992
anti-mCherry	Abcam	Cat# ab205402, RRID:AB_2722769
anti-chicken Alexa Fluor 488 conjugate	Thermo Fisher Scientific	Cat# A32931, RRID:AB_2762843
anti- guinea pig Alexa Fluor 647	Jackson Immunoresearch	Cat# 706-605-148, RRID:AB_2340476
anti- rabbit Alexa Fluor 647	Jackson Immunoresearch	Cat# 711-006-152, RRID:AB_2340586
Anti-GFAP-Cy3	Millipore-Sigma	Cat# C9205, RRID:AB_476889
Anti-rabbit Tyrosine Hydroxylase (TH)	Millipore-Sigma	Cat# AB152, RRID:AB_390204
Bacterial and virus strains		
AAV1-CaMK2-GCaMP6	Inscopix	Inscopix
AAV Gag Flex GcaMP6	Addgene	RRID:Addgene_100835
AAV hSyn Cre-P2A-tdTomato	Addgene	RRID:Addgene_107738
AAV-hSyn-DIO-hM3D(Gq)-mCherry	Addgene	RRID:Addgene_44361
pAAV-CAG-ArchT-tdTomato	Addgene	RRID:Addgene_29778
pCAG-iRFP670	Addgene	RRID:Addgene_45457
rAAV2-retro helper	Addgene	RRID:Addgene_81070
pAAV2/9n	Addgene	RRID:Addgene_112865
pAdDeltaF6	Addgene	RRID:Addgene_112867
Chemicals, peptides, and recombinant proteins		
Paraformaldehyde 16%	Electron Microscopy Sciences	Cat# 15710-S
$NaHPO_4$	Millipore-Sigma	Cat# S0751
NaH_2PO_4	Millipore-Sigma	Cat# S0876
PBS	Gibco	Cat# 10010-023
Heparin	Millipore-Sigma	Cat# H6279
Tetrahydrofuran with BHT	Millipore-Sigma	Cat# 186562
Triethylamine	Millipore-Sigma	Cat# T0886
Histodenz	Millipore-Sigma	Cat# D2158
Sodium Azide	Millipore-Sigma	Cat# S2002
Ultrapure Urea	Millipore-Sigma	Cat# 15505
Diatrizoic Acid	Millipore-Sigma	Cat# D9268
N-Methyl-D-Glucamine	Millipore-Sigma	Cat# M2004
DBE	Millipore-Sigma	Cat# 108014
Triethanolamine	Millipore-Sigma	Cat# T350-4
Formamide	Millipore-Sigma	Cat# F9037
Trizma Base	Millipore-Sigma	Cat# T6066
DMSO	Thermo Fisher Scientific	Cat# 20688
Triton X-100	Millipore-Sigma	Cat# T9284
Tween 20	Fisher scientific	Cat# BP337-500
Tamoxifen	Millipore-Sigma	Cat# T5648
Fetal Bovine Serum	Gibco	Cat# 16000084
4-OH Tamoxifen	Tocris	Cat# 3412
Cargille oil	Cargille Labs	Cat# 16482

(*Continued on next page*)

Continued		
REAGENT or RESOURCE	SOURCE	IDENTIFIER
Experimental models: Cell lines		
HEK293FT	Invitrogen	Cat# R700-07
Experimental models: Organisms/strains		
C57BL/6J	Jackson Laboratories	Cat# JAX:000664, RRID:IMSR_JAX:000664
cFos-Cre^{ERT2}	Jackson Laboratories	Cat# JAX:021882, RRID:IMSR_JAX:021882
VGAT-IRES-Cre	Jackson Laboratories	Cat# JAX:028862, RRID:IMSR_JAX:028862
CaMK2-Cre	Jackson Laboratories	Cat# JAX:005359, RRID:IMSR_JAX:005359
GCaMP3	Jackson Laboratories	Cat# JAX:014538, RRID:IMSR_JAX:014538
tdTomato (Ai14)	Jackson Laboratories	Cat# JAX:007914, RRID:IMSR_JAX:007914
Msx1-Cre^{ERT2}	Dr. Carol Mason	(Lallemand et al., 2013)
Thy1-GFP-M	Dr. Josef Gogos	Cat# JAX:007788, RRID:IMSR_JAX:007788
Software and algorithms		
Imaris	http://www.bitplane.com/imaris/imaris.	Imaris (RRID:SCR_007370)
ImageJ	Schneider et al., 2012	https://imagej.nih.gov/ij/

RESOURCE AVAILABILITY

Lead contact

Further information and requests for resources and reagents should be directed to and will be fulfilled by the Lead Contact, Dr. Eric R. Kandel (erk5@columbia.edu).

Materials availability

All unique/stable reagents generated in this study are available from the Lead Contact without restriction. Further information and requests for resources and reagents should be directed to and will be fulfilled by the Lead Contact Dr. Eric R. Kandel (erk5@columbia.edu).

Data and code availability

- This paper does not report Standardized datatypes. All data reported in this paper will be shared by the lead contact upon request.
- This paper does not report code.
- Any additional information required to reanalyze the data reported in this paper is available from the lead contact upon request.

EXPERIMENTAL MODEL AND SUBJECT DETAILS

Animals

Mice were maintained under standard conditions approved by the Institutional Animal Care and Use Committee (IACUC) of Columbia University. Animals were housed in a specific pathogen–free animal house under a 12/12-hour light/dark cycle and were provided food and water ad libitum. All wild type mice C57Bl6 were purchased from Jackson Laboratories (3-16 weeks old) (RRID:IMSR_JAX:000664). cFos-Cre^{ERT2} (Luo) (RRID:IMSR_JAX:021882), VGAT-Cre, CaMK2-Cre, GCaMP3 and tdTomato (Ai14) (RRID:IMSR_JAX:007914) were purchased from Jackson Laboratories (3-16 weeks old). Msx1-Cre^{ERT2} mouse embryos were a generous gift from Dr. Carol A. Mason, Columbia University. Thy1-GFP-M mice were a generous gift from Dr. Josef Gogos, Columbia University. Male and female mice were used for all experimental testing. The IACUC of Columbia University Medical Center approved all experiments involving animals.

METHOD DETAILS

Light transmittance measurements

The transmittance of half brains cleared with Fast 3D Clear and FDISCO, was measured with a spectrophotometer (Spectronic 200, Thermo Scientific). The brains were placed in a glass cuvette filled with the indicated refractive index matching solution (immersion oil or DBE respectively). Light beam oriented perpendicular to the sagittal plane of the brain and passed through the central part of the

brains. Transmittance of light was measured from 400-890nm in 10 nm increments. Light beam size was 7mm. The blank value was measured using a cuvette filled with the indicated refractive index matching solution without sample tissues. Similar measurements were obtained using a second spectrophotometer (Ultrospec 2100 pro) with similar results.

Signal to noise ratio

To measure signal to noise ratio (SNR) we used GCaMP3-CaMK2 mice brain hemispheres cleared in parallel with Fast 3D Clear and FDISCO methods. Light sheet images were taken at 488 and 568nm from two different planes. Control and experimental areas used, were of the same size. Using ImageJ (Schmidt et al., 2012), we selected two different brain regions that were homogeneously labeled (hippocampus and entorhinal cortex) and measured the fluorescence intensity for 525/50 emission. To calculate SNR, we used the formula $SNR = \frac{(\text{avgForeground} - \text{avgBackground})}{\text{stdBackground.}}$.

Fluorescence quantification

To measure the fluorescence preservation of Fast 3D Clear we used four fluorophores (Fast Blue, GCaMP, tdTomato, and IRF670.) We calculated the fluorescence intensity in confocal images homogenously labeled in ImageJ using two different depths (z) at 1.2 and 1.8 mm from the top of each whole adult mouse brain (Figure 4). For all the measurements we used the same acquisition settings for all the brains (N=3-5 per condition). All values were normalized with neighboring regions that exhibited near zero fluorescence. The values were expressed as SNR $\left(SNR = \frac{(\text{avgForeground} - \text{avgBackground})}{\text{stdBackground.}}\right)$. For long term fluorescence preservation, we used 3-month-old GCaMP3-CaMK2 mice stored in Cargille oil at 4°C for 7 months and freshly perfused mice of the same genotype and age, which were stored in Cargille oil for 7 days (whole brains). We calculated the fluorescence intensity in confocal images, acquired using a 10x 0.4 NA objective type using two different depths (z) at 1.2 and 1.8 mm from the top of each whole adult mouse brain (N=3 per condition).

Perfusion and tissue preparation

Adult mice were anesthetized with a mixture of ketamine/xylazine (100/20 mg/kg) via intraperitoneal injection. Thereafter, the animals were transcardially perfused with 10 ml phosphate-buffered saline (PBS) and then followed by 30 ml of 4% paraformaldehyde (PFA) in 0.1M $NaHPO_4/NaH_2PO_4$ or in PBS, pH 7.4. The tissue samples (adult mouse brains) were dissected. For mouse embryo collection, the day of the vaginal plug was defined as embryonic day 0.5 (E0.5), and embryos (E18.5) were removed from anesthetized mothers and transcardially perfused with 4% PFA in PBS. All harvested samples were post fixed overnight at 4°C in 4% PFA and then rinsed 5-6 times with PBS before clearing. For tissue section collection, brains were sliced into 50 μm -thick coronal sections with a vibratome (Leica VT1000 S, Germany).

Fast 3D Clear protocol

Mice were perfused with ice cold 10 ml PBS and then with 30 ml 0.1M $NaHPO_4/NaH_2PO_4$ or PBS+4% PFA. In some cases, mice were perfused along with Heparin 10 U/ml in PBS, in order to remove background from blood vessels. Samples were post fixed in 4% PFA overnight at 4°C rotating, end over end. Samples were washed 4-5 times with PBS for 10 min each, followed by 2-3 washes with deionized water at room temperature.

Delipidation/Dehydration: Tissues were incubated with THF with BHT (Millipore-Sigma 186562) at 4°C without light exposure, rotating end over end with the following solutions: 50% THF (20ml) in water with 20 μl of triethylamine (pH 9.0) (Millipore-Sigma T0886) for 1 hour, 70% THF (20 ml) in water with 30 μl of triethylamine (pH 9.0) for 1 hour and 90% THF (20 ml) in water with 60 μl of triethylamine (pH 9.0) overnight (~12-16 hours). pH was measured using pH strips. 20 ml of THF solutions were enough to process 4-5 adult whole mouse brains. At this stage brains shrunk considerably.

Rehydration: After overnight incubation with 90% THF the process was reversed rehydrating the samples with: 70% THF (20 ml) in water with 30 μl of triethylamine (pH 9.0) for 1 hour and then with 50% THF (20 ml) in water with 20 μl of triethylamine (pH 9.0) for 1 hour. At this stage, previous shrinkage was reversed.

Finally, samples were washed with ddH20 4-5 times for 10 min each (up to 12h).

At this stage, all specimens became translucent. Specimen size expanded (~50%) after the water washes.

Clearing: Tissues were then transferred in an aqueous clearing solution.

For whole mice (p24) we removed most of the internal organs (spleen, liver intestine) and we used the exact same clearing procedure. Specimens were immersed in the same clearing solution with higher refractive index RI= 1.545, for three days.

For 3-month-old mice we used the same steps as stated above and increased the THF incubation times (50% and 70% THF to 12 hours and 90% THF to 24 hours). A good indication that the whole mouse is adequately processed is the shrinkage of the mouse brain while in the 90% THF.

Fast 3D Clear solution

The clearing solution consists of 48 g Histodenz (Millipore-Sigma D2158), 0.6 g of Diatrizoic Acid (Millipore-Sigma D9268), 1.0 g of N-Methyl-D-Glucamine (Millipore-Sigma M2004), 0.008 g of Sodium Azide (optional) for 40 ml of solution (0.02% w/v) (Millipore-Sigma S2002) and 10 g of Ultrapure Urea for 50 ml of solution (20% w/v) (Millipore-Sigma 15505). To prepare the solution

~20 mL distilled water was added in glass bottle with all the chemicals and the powders were dissolved using a stir bar, briefly heating at 37°C to speed up the process. The final volume of the solution is ~50 ml and the RI 1.512-1.515. Addition of 13 ml of water, instead of 20 ml, produces 40 ml of clearing solution with RI 1.545. Urea can be omitted if the samples are used for other downstream processes, such as antibody staining (as antibodies are sensitive to urea) resulting in a 40ml solution with RI of 1.553. The samples were incubated overnight at 37°C with Fast 3D Clear solution (3-5 ml for a whole adult mouse brain are enough) and rotated end over end. The samples were always submerged completely in the solution. After overnight incubation the samples were completely transparent and stored at 4°C protected from light.

FDISCO clearing

FDISCO was performed according to (Qi et al., 2019). Briefly, brains were dehydrated with THF solutions (mixed with dH_2O, pH adjusted to 9.0 with triethylamine) at a series of concentrations 50, 70, 80, and 100 volume % (twice or thrice). Pure DBE was used as a refractive index matching solution to clear tissue after dehydration. All steps were performed at 4°C with slight shaking. During clearing, the tissues were placed in glass chambers covered with aluminum foil in the dark.

RTF clearing

RTF was performed according to (Yu et al., 2018). Briefly, brains were incubated in RTF-R1, RTF-R2 and RTF-R3 sequentially. Incubation time was 16 hours in each solution. RTF solutions were prepared by mixing triethanolamine, formamide and distilled water by volume. RTF-R1: 30%TEA/40%F/30%W. (30% triethanolamine (TEA), 40% formamide (F), 30% water (W) solution). RTF-R2: 60%TEA/25%F/15%W mixture (60% triethanolamine (TEA), 25% formamide (F), 15% water (W) solution). RTF-R3: 70%TEA/15% F/15%W – (70% triethanolamine (TEA), 15% formamide (F), 15% water (W) solution.

Imaging

Specimens were imaged with confocal or light sheet microscopy in the clearing solution or they were transferred to Cargille immersion oil type A.

Confocal microscopy: Whole brains were submerged in Fast 3D Clear medium or immersion oil. The dorsal hippocampus and dentate gyrus were imaged with an inverted confocal fluorescence microscope (Olympus IX81) equipped with a 4x 0.16 NA Fluar and 10x 0.40 NA Plan-Apochromat objectives. The *z*-step interval was 4.76 μm, pinhole size 80-85μm (auto), PMT settings 600-700 and laser power from 5%-25% depending on the fluorophore. Acquisition settings were 1600X1600 and 10p/sec. We also tested Fast 3D Clear using a W1-SoRa-Yokogawa inverted spinning disk confocal microscope using 10x 0.45 NA Plan-Apochromat objective. For spine visualization we used an XA1R confocal microscope with a 20x 0.95 NA Plan-Apochromat objective. Briefly, 0.5 μm optical sections were acquired in 100μm tissue volume. Laser settings were first tested using unlabeled cleared brains to ensure that no autofluorescence in any wavelength was present. All samples were protected from ambient light. Imaris software was used to produce 3D visualization of cleared samples.

Light sheet fluorescence microscopy: Brain samples were imaged using a light sheet fluorescence microscope (UltraMicroscope II Light Sheet Microscope, Miltenyi Biotec, Germany) equipped with an sCMOS camera (Andor Neo), a 2x 0.5 NA Olympus VMPLAPO Plan Apochromat objective lens equipped with a correction lens , and an Olympus MVX10 zoom microscope body. The cleared tissues were mounted on the sample holder and imaged in Cargille immersion oil type A with refractive index R=1.515 (Cargille 16842) in the sample reservoir. Some samples were embedded in 4% low melting agar in the Fast 3D Clear solution and then visualized with confocal or light sheet microscopy. For scanning of whole brains and image acquisition from regions of interest, the *z*-step interval ranged from 4-7μm and the laser power to 5%-25% depending on the fluorophores. Other parameters were: sheet width from 30-100%, dynamic focus from 4-17 depending on the zoom setting and exposure time 100ms. For Imaging tdTomato and IRF fluorophores laser 605/52 and 705/72 were used with laser intensities reaching up to 25% of laser power.

These parameters were tested using unlabeled brains that produced no signal at 30% laser power. Samples in immersion oil (RI~1.515) or clearing solution can be stored at 4°C protected from light, for at least 6 months (time observed). For 3D visualization, Imaris software was used. None of the figures were processed with algorithms for better visualization, except from the spine images in which a deconvolution algorithm was used.

Immunohistochemistry

Coronal sections (50 μm) along the entire rostrocaudal extension of the hippocampus were cut on a vibratome and stored in 0.1 M Tris pH 7.4, 30% ethylene glycol, and 30% glycerol at −20°C until further processed. Immunofluorescence was performed on every fifth section. Sections were washed 3 times with 0.1 M Tris pH 7.4, 0.15 M NaCl and 0.3% Triton X-100 (TBSTX) at room temperature. Sections were additionally washed 3 times with TBSTX buffer and blocked for 1 hour at room temperature in blocking buffer (TBSTX supplement with mouse IgG (1 μg/ml) and 1% BSA to reduce non-specific binding of mouse antibodies). Primary antibodies were incubated at 4°C for 24 to 48 hours. After primary antibody incubation, sections were washed at least 3-5 times with TBSTX buffer and incubated with the appropriate Alexa fluorescent secondary antibodies (Invitrogen). Sections were washed 3-5 times with TBSTX buffer and then mounted on Superfrost slides (Fisher Scientific) with Slow fade Diamond mounting solution (Invitrogen) or directly to 3D Clearing solution. Antibodies used: DCX 1:500 Millipore (AB2253), anti-mCherry (Abcam Cat# ab205402, RRID: AB_2722769), Alexa Fluor 488 conjugate (Thermo Fisher Scientific) and Alexa Fluor 647 (Jackson Immunoresearch).

Stereotaxic injections were performed as described previously (Kosmidis et al., 2018). Mice were anaesthetized with a Ketamine/Xylazine mixture (100 mg/kg) and (20 mg/kg) respectively. Injections were targeted unilaterally to the dentate gyrus (dentate mainly) (−1.96 mm anteroposterior (AP), ± 1.28 mm mediolateral (ML), −1.98 mm dorsoventral (DV)), the Ent/Prh (−3.15 mm anteroposterior (AP), ± 4.3 mm mediolateral (ML), −3.65 mm dorsoventral (DV)) or S1DZ (−1.0 mm anteroposterior (AP), ± 1.28 mm mediolateral (ML), −0.5 mm dorsoventral (DV)). Injection volumes ranged from 250-500 nl and contained rAAV2, AAV1 viral particles or Fast Blue 0.2 mg/ml (Polysciences 17740). Injection time was 10 min. After the injection the needle remained in place for another 10 min before it was withdrawn.

Immunolabeling protocol (iDISCO)

A shorter Fast 3D Clear protocol was applied to hippocampi prior to immunolabeling with the steps described in the iDISCO protocol. Hippocampi from GCaMP3-CaMK2 mice were freshly dissected and fixed in 4% PFA for 20 min in room temperature. Hippocampi were transferred sequentially to 50% and 70% THF solution for 20 min each, and then to 90% THF for 2h at 4°C, Rehydration was achieved after 20 min in 70% and then 50% THF solution. After several washes with water at 4°C protected from light the dissected hippocampi were immersed in Fast 3D Clear solution, at 37°C until cleared (2 hours minimum). Wholemount staining performed according to (Renier et al., 2014) in the same hippocampi. Briefly, reversed cleared GCaMP3-CaMK2 hippocampi incubated in PBS/0.2% Triton X-100/20% DMSO/0.3 M glycine at 37°C for 2 hours, then blocked in PBS/0.2% Triton X-100/10% DMSO/6% Fetal Bovine Serum (FBS) at 37°C for 12 hours. Samples were washed in PBS/0.2% Tween-20 with 10 μg/ml heparin (PTwH) for 1 hour twice, then incubated in primary antibody (DCX-1:250 dilution) in PTwH/5% DMSO/3% FBS at 37°C for 24 hours. Samples were then washed in PTwH 3 times for 15 min, then incubated in Alexa-647 secondary antibody at 1:500 dilution in PTwH/3% FBS at 37°C for 12 hours. Samples were finally washed in PTwH 3 times for 15 min each before clearing and imaging. For half brains we used the same protocol as above. Briefly, we first performed Fast 3D Clearing with Urea and imaged the brains. Then we reversed clearing with PBS and distil water washes for 16 hours at 4°C (4-5 washes). Then we followed the iDISCO staining protocol as above, by extending the incubation times with primary and secondary antibodies for 5 days with constant rotation (20rpm) at 37°C. During the washes (2∼hours) we included a washing step with water to create tissue expansion to presumably aid the antibody penetration. We found that lightly damaged half brains have better and faster antibody penetration than intact ones. The half brains were cleared with Fast 3D Clearing solution without Urea in order to better preserve fluorescent staining.

For half brains we used mouse GFAP-Cy3 (Sigma C9205) and rabbit TH (Millipore AB152) antibodies at 1:250 dilution.

Tamoxifen (TAM)

cFos-Cre^{ERT2}-tdTomato animals aged 8–12 weeks were administered 5 mg of tamoxifen (Sigma), suspended in 100 μl 1:1 honey: water mixture by gavage once a day, at least 12 hours apart according to Kosmidis et al., 2018. cFos-Cre^{ERT2}-tdTomato received 2 doses of 5 mg Tamoxifen prior to any other experimental manipulations. For Msx1-Cre induction in mouse embryos, the pregnant mother was injected with 3 doses of 4-hydroxy tamoxifen (2 mg) given at E13.5, E14.5 and E15.5.

Contextual fear conditioning in cFos-Cre^{ERT2}-tdTomato mice

Mice were exposed for 4 min to the training context A in which they received 3-foot shocks of 0.7 mA for 2 sec, 1 min apart (Learning). Mice received 2 doses of tamoxifen orally (once every 8 hours) and 24 hours later they were exposed to the same context without any shock (Kosmidis et al., 2018). Five days later mice were processed for Fast 3D Clear.

HEK293FT cell culture, transfection, and production of rAAV2 and AAV

HEK293FT were purchased from Life Sciences and cultured according to manufacturer's instructions (R700-07). Viral particles were produced using the HEK293FT cell line according to standard procedures in a BSL-2 safety cabinet according to AAV production protocol. Plasmid vectors that were used: rAAV2-retro helper was a gift from Alla Karpova & David Schaffer (Addgene plasmid # 81070; http://n2t.net/addgene:81070; RRID:Addgene_81070), pAdDeltaF6 was a gift from James M. Wilson (Addgene plasmid # 112867 ; http://n2t.net/addgene:112867 ; RRID:Addgene_112867), pAAV2/9n was a gift from James M. Wilson (Addgene plasmid # 112865 ; http://n2t.net/addgene:112865 ; RRID:Addgene_112865), pAAV-CAG-ArchT-tdTomato was a gift from Edward Boyden (Addgene plasmid # 29778 ; http://n2t.net/addgene:29778 ; RRID:Addgene_29778), pCAG-iRFP670 was a gift from Wilson Wong (Addgene plasmid # 45457 ; http://n2t.net/addgene:89687 ; RRID:Addgene_89687). The viral titers were 10^{12}/ml. AAV1-CaMK2-GCaMP6 virus particles were purchased from Inscopix. AAV Gag Flex GcaMP6 (Addgene_100835), AAV hSyn Cre-P2A-tdTomato (Addgene_107738) and pAAV-hSyn-DIO-hM3D(Gq)-mCherry (Plasmid #44361) plasmids were also purchased from Addgene.

QUANTIFICATION AND STATISTICAL ANALYSIS

Statistics were performed with GraphPad Prism 8 software. Repeated-measures ANOVA (Tukey) and t tests were used as indicated. The results are presented as mean ± SEM. Statistical significance was set at $p < 0.05$ (*$p < 0.05$, **$p < 0.01$, and **$p < 0.001$). Statistical details of experiments, including the statistical tests used, exact value of n (number of animals), and exact p values can be found in figure legends of Figures 1, S1, and S2.